View Article Online
View Journal

Dalton Transactions

An international journal of inorganic chemistry

Accepted Manuscript

This article can be cited before page numbers have been issued, to do this please use: S. Mandal, E. Y. Song, T. J. Emge, F. Hasanayn and A. S. Goldman, *Dalton Trans.*, 2026, DOI: 10.1039/D6DT00920D.

ROYAL SOCIETY OF CHEMISTRY

rsc.li/dalton

View Article Online
DOI: 10.1039/D6DT00920D

COMMUNICATION

A metal-metal quadruply bonded dimer of two pincer-ligated metal centers

Souvik Mandal,[a] Ethan Y. Song,[a] Thomas J. Emge,[a] Faraj Hasanayn*[b] and Alan S. Goldman*[a]

Received 00th January 20xx,
Accepted 00th January 20xx

DOI: 10.1039/x0xx00000x

Reduction of the pincer complex ($P^{Ar}NP$)$MoBr_3$ using Na/Hg under argon yields a quadruply bonded Mo-Mo dimer, (κ^3-$P^{Ar}NP$)BrMo≣Mo(κ^3-$P^{Ar}NP$)Br. The complex represents a rare example of a metal-metal bonded species in which both metal centers bear a κ^3-*mer* coordinated pincer ligand.

Complexes with metal-metal bonds comprise one of the most intensively studied classes of coordination compounds.[1-4] The metal-metal quadruple bond, in particular, has fascinated chemists since first reported by Cotton in 1964.[5-6]

The field of pincer ligands has seen explosive growth over the past two to three decades. Interest stems from the great tunability that pincer ligands offer with respect to both steric and electronic factors, the ease and modularity of their syntheses, and the high stability of their complexes, attributable to multidentate bonding.[7-9] These properties lead to numerous applications in diverse fields including catalysis and optoelectronics.[10-15]

Despite the breadth of these two classes of coordination complexes – metal–metal bonds and pincer-ligated systems – there has been little overlap between them. In particular there have been remarkably few reports of metal–metal bonded complexes in which both metals are κ^3-pincer-ligated. To our knowledge, the only such examples (all reported quite recently) are Pt-Pt complexes in which each Pt center bears a planar κ^3 NCN- or NNC-type ligand.[16-18] These planar pincer ligands impose minimal steric hindrance, while the Pt-Pt bonds are quite long (>3.0 Å) and are supported by an ancillary ligand bridging the two Pt centers. Being the only examples of the (pincer)M–M(pincer) motif, these complexes might suggest that shorter metal-metal bonds and more "classical" pincer ligands[19] (those with bulky terminal coordinating groups e.g. PR_2 or NR_2) would represent a highly unfavorable combination. Herein, however, we report a complex in which both Mo centers are ligated by a relatively bulky "classical" pincer, Ozerov's bis (2-(diisopropylphosphino)-4-methylphenyl)amide ($P^{Ar}NP$)[20], yet are linked by a short (2.17 Å) Mo-Mo quadruple bond.

There are over 1500 structurally characterized examples of metal–metal quadruply-bonded species reported in the 2025 Cambridge Structural Database[21], the majority of which (over 900) are Mo–Mo complexes. In all but about 80 cases, one or more bridging ligands are present and the non-bridging ligands are monodentate. Among the few complexes with tridentate ligands, in all but one case they are bridging, coordinating in a κ^2 fashion to one Mo center and κ^1 to the second (e.g. Scheme 1a).[22-25] To date, only a single exception has been reported. In 2002, Walton and co-workers described a Mo≣Mo complex in which a pyridine-based PNP ligand is κ^3-coordinated to one of the two Mo centers (Scheme 1b).[26]

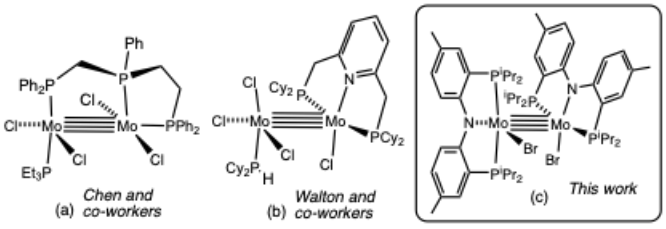

Scheme 1 Examples of Mo≣Mo complexes bearing tridentate ligands

We recently reported the binding and splitting of dinitrogen by two ($P^{Ar}NP$)MoX fragments by reaction of **$LMoBr_3$** (L = $P^{Ar}NP$) with sodium amalgam under nitrogen atmosphere (Scheme 2a).[27] When 2 equiv sodium amalgam is added to a THF-d_8 solution of **$LMoBr_3$** under argon atmosphere rather than under dinitrogen (Scheme 2b), upon vigorous shaking the color changes from green to dark purple and the ^{1}H NMR spectrum reveals the complete loss of **$LMoBr_3$** with formation of a new diamagnetic product. This species is unreactive toward added N_2, or even toward PMe_3 or CO. The $^{31}P\{^1H\}$ NMR spectrum of the product mixture displays an AB doublet at 37.0 and 29.5 ppm with $^2J_{PP}$ = 104 Hz. Crystals were obtained by diffusion of pentane into a saturated THF solution of the product, and X-ray

[a] Department of Chemistry and Chemical Biology, Rutgers, The State University of New Jersey, New Brunswick, New Jersey 08854, USA. E-mail: alan.goldman@rutgers.edu
[b] Department of Chemistry, American University of Beirut, Beirut 1107 2020, Lebanon. E-mail: fh19@aub.edu.lb

diffractometry reveals a Mo-Mo unit in which each Mo center bears a P^{Ar}NP pincer ligand and a bromide, complex **1** (Scheme 2b; Fig. 1).

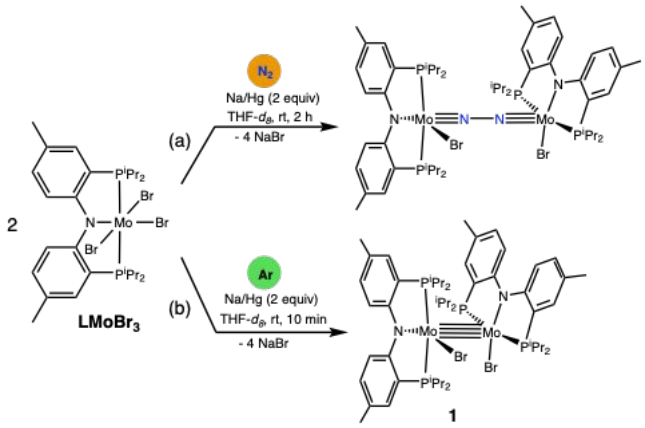

Scheme 2 Two electron reduction of **LMoBr$_3$** yielding complex **1**

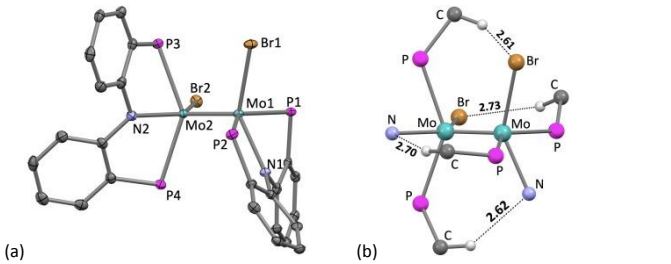

Fig. 1 (a) Thermal ellipsoid representation (50% probability ellipsoids) of the structure of **1** in the solid state. Hydrogen atoms, methyl groups on the aryl ring, and isopropyl groups on the phosphorus atoms omitted for clarity. (b) Structure of **1** with only Mo, Mo-bound atoms, and phosphine methine groups syn to the opposing Mo center, with short CH–Br/N distances given (Å).

Table 1 gives selected X-ray crystallographic bond distances in **1** and compares them with those optimized using the M06 density functional in the gas phase, starting with the experimental structure. The non-metals carried the 6-311G(d,p) basis set, while molybdenum carried the SDD relativistic ECP and corresponding basis set. (See the SI for computational details). The crystallographic Mo–Mo bond length in **1** is 2.172 Å, at the upper end of the normal range of Mo–Mo quadruple bond lengths, 2.06–2.17 Å.[1, 6] The calculated bond length, 2.166 Å, is in good agreement with the experimental value.

Table 1 Selected bond distances of **1** and comparison with the optimized structure

Bond distances (Å)	**2** (XRD)	**DFT optimized** [a]
Mo1-Mo2	2.172	2.166
Mo1-N1	2.191	2.180
Mo2-N2	2.164	2.198
Mo1-P1	2.532	2.559
Mo1-P2	2.521	2.582
Mo2-P3	2.538	2.553
Mo2-P4	2.551	2.561
Mo1-Br1	2.569	2.623
Mo2-Br2	2.544	2.625

The two *i*-Pr substituents on each pincer ligand that are *syn* to the Mo-Mo bond occupy essentially equatorial positions of the 5-membered metallacyclic rings. This arrangement minimizes steric crowding between the two units, while bringing the methine CH bonds to within approximately 2.7 Å of the bromo or amido ligand centers of the opposing metal center, suggesting some degree of hydrogen-bonding (Fig. 1b).[28-29] The ^{1}H NMR spectrum of **1** in THF indicates that the structural features of the ligands observed in the solid state are retained in solution. Specifically, four multiplets are observed at δ 4.65, 2.84, 2.23, and 1.50 ppm, corresponding to four *i*-Pr methine protons in very different environments.

An NBO analysis identifies one σ, two π, and one δ occupied MO in the Mo-Mo bond (Fig. 2) with predominantly metal d-character (>85%). Thus our experimental and computational results are fully consistent with a Mo-Mo quadruple bond in **1**.[1, 6]

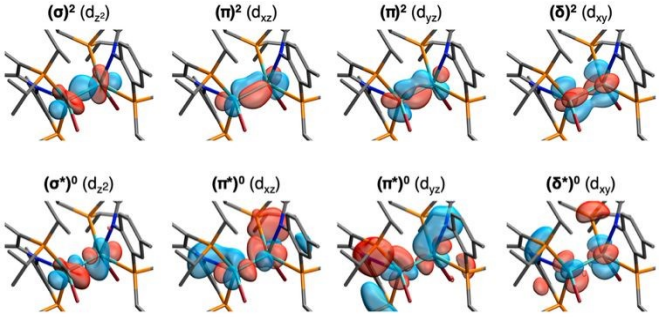

Fig. 2 Doubly occupied bonding and empty antibonding NBOs of the Mo–Mo core of **1**.

Given the unprecedented nature of a metal-metal bonded complex composed of two metal fragments with non-planar pincer ligands, it seemed surprising to find a system combining a relatively bulky pincer ligand with a particularly short M–M distance characteristic of a metal-metal quadruple bond. We considered whether features specific to the P^{Ar}NP ligand, such as the H-bonding between metal centers discussed above, might strongly favor dimerization. To probe this possibility, hypothetical analogues with phenyl-based pincer ligands, ^{iPr}PCP and ^{iPr}POCOP were investigated computationally. For this purpose, final electronic and solvation free energies were obtained by single point calculations in a polarisable continuum representing THF as solvent on the gas-phase geometries using the M06-D3 density functional and a def2 basis set as described in the SI. These calculations rule out a unique stabilizing role of P^{Ar}NP: the computed Mo–Mo bond strengths in [(^{iPr}PCP)MoBr]$_2$ and [(^{iPr}POCOP)MoBr]$_2$ (Scheme 3) are actually slightly *greater* than that calculated for **2** (see SI).‡

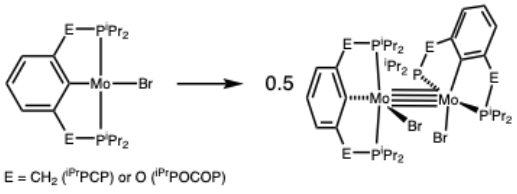

Scheme 3 Computationally investigated Mo-Mo quadruply bonded dimers

Surprisingly, when the reduction of **LMoBr$_3$** under argon was carried out with 2 equiv KC_8 instead of Na/Hg, complex **1** was not formed. Instead, the ^{1}H NMR spectrum indicated rapid

formation of a paramagnetic species that was stable at room temperature for at least 20 days. The magnetic susceptibility of the product was determined by the Evans method to be 4.6 μ_B, indicating a quintet ground spin state. Our initial experimental and computational investigations suggest this species is a THF adduct of the (P^{Ar}NP)MoBr fragment **LMoBr(THF)$_n$**, Scheme 4.

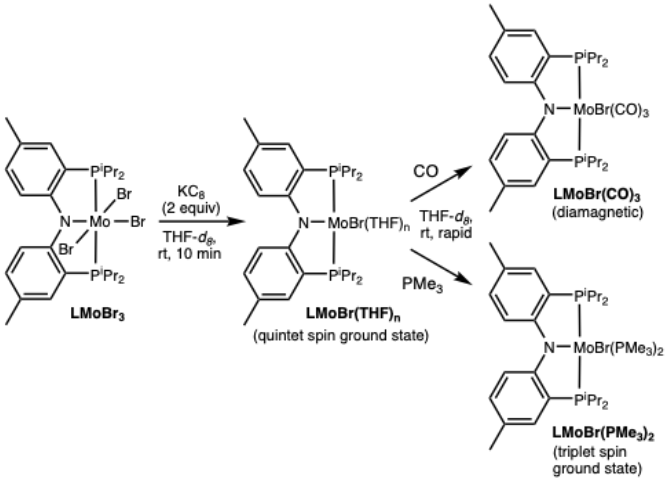

Scheme 4 Formation of **LMoBr(THF)$_n$** using KC_8, and its trapping with CO or PMe_3

Attempts to trap the putative species **LMoBr(THF)$_n$** support its formulation as a solvated form of the **LMoBr** fragment. Upon addition of 1 atm CO, a THF solution immediately changed from purple to red, and a diamagnetic species was observed by ^{1}H and ^{31}P{^{1}H} NMR spectroscopy. When the reaction was performed with ^{13}CO, the ^{31}P{^{1}H} and ^{13}C{^{1}H} NMR spectra clearly demonstrated the formation of a (P^{Ar}NP)Mo species with three inequivalent CO ligands and two inequivalent P^{i}Pr$_2$ groups (see SI). These spectra are readily assigned to the seven-coordinate complex **LMoBr(CO)$_3$** (Scheme 4), which is well precedented by Kirshner's halotricarbonyl molybdenum complexes.[30-31] Attempts to crystallize this species were unsuccessful.

Addition of 2 equiv of PMe_3 to a solution of **LMoBr(THF)$_n$** resulted in an immediate color change from purple to magenta. In contrast to the reaction with CO, the resulting ^{1}H NMR spectrum was indicative of a paramagnetic species, assigned as **LMoBr(PMe$_3$)$_2$** (Scheme 4). The magnetic susceptibility, measured by the Evans method, was 2.9 μ_B, consistent with a triplet ground state.

Ligand binding to **LMoBr** was computationally investigated. Coordination of two THF molecules is calculated to be exothermic by 17.8 kcal/mol, affording ***trans*-LMoBr(THF)$_2$** with a quintet ground state (although with an enthalpy only 1.0 kcal/mol lower than the corresponding triplet). Coordination of CO or PMe_3 was calculated to be much more exergonic, yielding **LMoBr(CO)$_3$** and ***trans*-LMoBr(PMe$_3$)$_2$** which are computed to have singlet and triplet ground states, respectively. These results (Table 2) are fully consistent with the experimental NMR and magnetic susceptibility data.

Table 2 Thermodynamics of ligand binding and dimerization of **LMoBr** [a]

Complex	Spin state	ΔH	ΔG
LMoBr	quintet	0.0	0.0
***trans*-LMoBr(THF)$_2$**	triplet	-16.8	-10.7
***trans*-LMoBr(THF)$_2$**	quintet	-17.8	-12.6
***cis*-LMoBr(THF)$_2$**	triplet	-13.3	-8.3
LMoBr(THF)•THF [b]	quintet	-19.0	-16.2
***trans*-LMoBr(CO)$_2$**	singlet	-60.3	-35.8
***cis*-LMoBr(CO)$_2$**	singlet	-66.4	-40.5
LMoBr(CO)$_3$	singlet	-81.2	-44.0
***trans*-LMoBr(PMe$_3$)$_2$**	triplet	-39.2	-22.5
***cis*-LMoBr(PMe$_3$)$_2$**	triplet	-38.0	-21.3
dimerization: 0.5 **1**	singlet	0.5•(-51.6)	0.5•(-33.4)

[a] Gibbs free energies and enthalpies computed at the M06-D3/def2 level in THF continuum and reported in kcal/mol with respect to the calculated energy of **LMoBr** (with the formation of 0.5 mol **2** indicated as 0.5 times the total values for 1.0 mol **2**). Values of ΔG for formation of THF complexes are derived with a statistical correction to account for the concentration of THF solvent, 10.0 M (244.7 atm) and scaling of the rotational and translational entropy components by a factor of 0.5[32-34]; see SI. [b]Attempts to optimize a quintet state of ***cis*-LMoBr(THF)$_2$** led to the decoordination of one THF ligand and to a complex **LMoBr(THF)•THF** in which the O atom of the non-coordinated THF molecule is H-bonded to an α-C-H bond of the coordinated molecule of THF.

The assignment of **LMoBr(THF)$_2$** as the paramagnetic species formed upon reaction of **LMoBr$_3$** with KC_8 has important mechanistic implications, namely that dimer **1** does not form via direct dimerization of monomeric **LMoBr**. Use of the highly effective reductant KC_8 leads to rapid and quantitative reduction of **LMoBr$_3$** to give **LMoBr(THF)$_2$**. While further mechanistic studies are required, we speculate that when the less effective reductant Na/Hg is employed, the reduction of **LMoBr$_3$** is sufficiently slow to allow reaction with the initially formed **LMoBr(THF)$_2$**. An alternative possibility is that the presumed initial reduction product, **LMoBr$_2$(THF)**, is very rapidly reduced by KC_8 to give **LMoBr(THF)$_2$**, whereas reduction by Na/Hg is slow enough to permit **LMoBr$_2$(THF)** to undergo dimerization. In either case, reaction of **LMoBr$_3$** with Na/Hg generates a complex with a Mo_2Br_4 core, which is subsequently reduced to form complex **2** (Scheme 5). At present we favor the former pathway, as DFT calculations indicate that reaction of **LMoBr(THF)$_2$** with **LMoBr$_3$** is thermodynamically much more favorable (ΔG = -0.6 kcal/mol) than dimerization of **LMoBr$_2$(THF)** (ΔG = 19.6 kcal/mol).

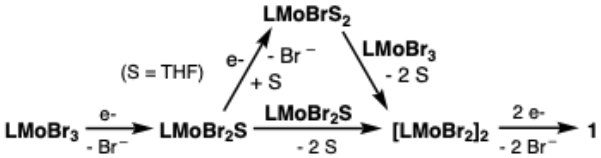

Scheme 5 Possible pathways for the formation of **2**

In summary, a metal fragment bearing a typical (relatively bulky and non-planar) pincer ligand has been found to undergo dimerization to ultimately form a metal-metal quadruply bonded complex. Computational studies suggest that such dimerizations are thermodynamically favorable more generally. In light of the extensive interest in both metal-metal bonded complexes and pincer-ligated complexes, this points to a broad and unexplored class of bimetallic pincer complexes.

Conflicts of interest

There are no conflicts to declare.

Data availability

The data supporting the findings of this study are available within the article and its supplementary information (SI). Supplementary information: experimental procedures and characterizations, crystallographic data, NMR spectra, computational methods and results. Optimized structures for calculated species (.mol format) (ZIP). CCDC 2457509, 2459044, 2515783 and 2516137 contain the full supplementary crystallographic data for this paper.

Acknowledgements

This work was supported through the National Science Foundation Chemical Catalysis program under Grant No. CHE-2247259. F. H. acknowledges support from the Mamdouha El-Sayed Bobst funds of AUB. Prof. Oleg Ozerov (Texas A&M University) is thanked for helpful discussions and a gift of $P^{Ar}NP$ synthetic precursor.

Notes and references

‡ Isodesmic reactions were calculated in which PH_2 and P^iPr_2 groups were exchanged between complex **2** and the analogous ^{R}PCP- and ^{R}POCOP-ligated dimeric complexes and analogues truncated with PH_2 groups. The computed energies indicated that the $P^{Ar}NP$ backbone did not confer any particular relief (relative to ^{R}PCP or ^{R}POCOP) of steric repulsion between the quadruply bonded metal centers (see SI).

1. H. Vahrenkamp, *Angew. Chem., Int. Ed.*, 1978, **17**, 379-392, doi: 10.1002/anie.197803793.
2. P. Buchwalter, J. Rosé and P. Braunstein, *Chem. Rev.*, 2015, **115**, 28-126, doi: 10.1021/cr500208k.
3. J. F. Berry and C. C. Lu, *Inorg. Chem.*, 2017, **56**, 7577-7581, doi: 10.1021/acs.inorgchem.7b01330.
4. R. H. Duncan Lyngdoh, H. F. Schaefer, III and R. B. King, *Chem. Rev.*, 2018, **118**, 11626-11706, doi: 10.1021/acs.chemrev.8b00297.
5. F. A. Cotton, N. F. Curtis, C. B. Harris, B. F. G. Johnson, S. J. Lippard, J. T. Mague, W. R. Robinson and J. S. Wood, *Science*, 1964, **145**, 1305-1307, doi: 10.1126/science.145.3638.1305.
6. F. A. Cotton, C. A. Murillo and R. A. Walton, eds., *Multiple bonds between metal atoms*, Springer Science & Business Media, New York, 2006.
7. G. van Koten, D. Milstein and Editors, *Organometallic Pincer Chemistry*, Springer GmbH, 2013.
8. E. Peris and R. H. Crabtree, *Chem. Soc. Rev.*, 2018, **47**, 1959-1968, doi: 10.1039/C7CS00693D.
9. D. Morales-Morales, ed., *Pincer Compounds: Chemistry And Applications*, Elsevier B.V., Amsterdam, 2018.
10. M. Albrecht and D. Morales-Morales, *Iridium Complexes in Organic Synthesis*, 2009, 299-323, doi:
11. K. J. Szabo, *Top. Organomet. Chem.*, 2013, **40**, 203-242, doi: 10.1007/978-3-642-31081-2_7.
12. G. van Koten and R. A. Gossage, eds., *The Privileged Pincer-Metal Platform: Coordination Chemistry & Applications*, in *Top. Organomet. Chem., 54*, Springer GmbH, 2016.
13. A. Kumar, T. M. Bhatti and A. S. Goldman, *Chem. Rev.*, 2017, **117**, 12357-12384, doi: 10.1021/acs.chemrev.7b00247.
14. K. Das and A. Kumar, *Adv. Organomet. Chem.*, 2019, **72**, 1-57, doi: 10.1016/bs.adomc.2019.02.004.
15. V. Arora, H. Narjinari, P. G. Nandi and A. Kumar, *Dalton Trans.*, 2021, **50**, 3394-3428, doi: 10.1039/D0DT03593A.
16. M. A. Esteruelas, S. Moreno-Blázquez, M. Oliván and E. Oñate, *Inorg. Chem.*, 2024, **63**, 14482-14494, doi: 10.1021/acs.inorgchem.4c01712.
17. R. A. Shilov, I. S. Podkorytov, K. S. Kisel, E. E. Galenko, D. O. Karpitskaya, I. A. Rodionov, J. R. Shakirova and S. P. Tunik, *Inorg. Chem.*, 2024, **63**, 11194-11208, doi: 10.1021/acs.inorgchem.4c00984.
18. A. Yu, W. Jiang, Y. Shen and Y. Zhang, *Cryst. Growth Des.*, 2025, **25**, 1872-1879, doi: 10.1021/acs.cgd.4c01747.
19. M. Vogt and R. Langer, *Eur. J. Inorg. Chem.*, 2020, **2020**, 3885-3898, doi: 10.1002/ejic.202000513.
20. L. Fan, B. M. Foxman and O. V. Ozerov, *Organometallics*, 2004, **23**, 326-328, doi: 10.1021/om034151x.
21. C. R. Groom and F. H. Allen, *Angew. Chem., Intl. Ed.*, 2014, **53**, 662-671, doi: 10.1002/anie.201306438.
22. F. A. Cotton and B. Hong, *Inorg. Chem.*, 1993, **32**, 2354-2359, doi: 10.1021/ic00063a026.
23. C.-T. Lee, S.-F. Chiang, C.-T. Chen, J.-D. Chen and C.-D. Hsiao, *Inorg. Chem.*, 1996, **35**, 2930-2936, doi: 10.1021/ic951187b.
24. C.-T. Lee, W.-K. Yang, J.-D. Chen, L.-S. Liou and J.-C. Wang, *Inorg. Chim. Acta*, 1998, **274**, 7-14, doi: 10.1016/S0020-1693(97)05961-6.
25. M.-C. Suen, S.-F. Chiang, J.-D. Chen, S.-S. Chern and C.-D. Hsiao, *J. Chin. Chem. Soc.*, 1998, **45**, 263-268, doi: 10.1002/jccs.199800042.
26. H.-F. Lang, P. E. Fanwick and R. A. Walton, *Inorg. Chim. Acta*, 2002, **329**, 1-8, doi: 10.1016/S0020-1693(01)00787-3.
27. S. Mandal, S. Malakar, R. N. Allen, A. Tyryshkin, T. J. Emge, F. Hasanayn and A. S. Goldman, *ChemRxiv*, 2025, doi: 10.26434/chemrxiv-2025-40qzq.
28. M. Domagała and S. J. Grabowski, *J. Phys. Chem. A*, 2005, **109**, 5683-5688, doi: 10.1021/jp0511496.
29. Y. Gu, T. Kar and S. Scheiner, *J. Molec. Struct.*, 2000, **552**, 17-31, doi: 10.1016/S0022-2860(00)00455-5.
30. S. R. M. M. de Aguiar, B. Stöger, E. Pittenauer, M. Puchberger, G. Allmaier, L. F. Veiros and K. Kirchner, *J. Organomet. Chem.*, 2014, **760**, 74-83, doi: 10.1016/j.jorganchem.2013.12.018.
31. D. Benito-Garagorri, E. Becker, J. Wiedermann, W. Lackner, M. Pollak, K. Mereiter, J. Kisala and K. Kirchner, *Organometallics*, 2006, **25**, 1900-1913, doi: 10.1021/om0600644.
32. T. D. Lohrey, A. Q. Cusumano, W. A. Goddard, III and B. M. Stoltz, *ACS Catal.*, 2021, **11**, 10208-10222, doi: 10.1021/acscatal.1c02790.
33. A. V. Finkelstein and J. Janin, *Protein Eng.*, 1989, **3**, 1-3, doi: 10.1093/protein/3.1.1.
34. Y.-i. Izato, A. Matsugi, M. Koshi and A. Miyake, *Phys. Chem. Chem. Phys.*, 2019, **21**, 18920-18929, doi: 10.1039/C9CP03226F.

View Article Online
DOI: 10.1039/D6DT00920D

A metal-metal quadruply bonded dimer of two pincer-ligated metal centers

Souvik Mandal,[a] Ethan Y. Song,[a] Thomas J. Emge,[a] Faraj Hasanayn*[b] and Alan S. Goldman*[a]

Data availability statement

The data supporting the findings of this study are available within the article and its supplementary information (SI). Supplementary information: experimental procedures and characterizations, crystallographic data, NMR spectra, computational methods and results. Optimized structures for calculated species (.mol format) (ZIP).

CCDC 2457509, 2459044, 2515783 and 2516137 contain the full supplementary crystallographic data for this paper.